FREQUENCY ANALYSIS OF 3-D WOVEN COMPOSITE UNDER STATIC AND IMPULSIVE COMPRESSION

Baozhong Sun, Bohong Gu
College of Textiles, Donghua University, Shanghai, P.R.China, 200051

Abstract

The Z-transform theory of discrete system is applied to 3-D angle-interlock woven structural composites for characterizing the relationship between strain-time history and stress-time history under static (strain rate: 0.001/s) and impulsive (strain rate up to 2700/s) compression along in-plane direction and out-of-plane direction respectively. The good agreement between the fitted compression stress-strain curves from the difference equation of discrete system and experimental curves proves the validation of investigating the strain rate effect of compression behaviors assuming the composite is a discrete system. The transfer function of the system which derived from the Z-transform is used to analyze the dynamic response and stability of the composites with different preform structures and loading conditions. The factors of the compression strain rate and composite microstructure which influence the stability of the discrete system have been discussed. The discrete system becomes more stable as the strain rate increases. However, the stability of the system will decrease when the compressive deformation (i.e., strain) increases in the composites. The combined effect of the two factors deduced the complex phenomenon of frequency responses and stability at different strain rates. This is a first attempt to discuss compression behavior of the 3-D woven structural composites at quasi-static and high strain rate states under frequency domain in order to disclose the relationships between mechanical behavior and features of frequency responses. Further studies will be conducted to investigate the relationships among features of frequency responses, microstructure of the composites, loading condition and testing methods for the 3-D woven structural composites under quasi-static and high strain rate compressions in detail.

1 Introduction

Three-dimensional woven structural composites have been widely used in impact resistance because of the higher impact damage tolerance and fracture toughness than laminates. The responses of the 3-D woven composites under different strain rate loadings vary with fabric architectures and loading conditions. Ko et al [1] compared the impact behavior of glass/epoxy composites. Gong et al [2] tested the sub-perforation velocity impact of 3-D braided composites and quasi-isotropic laminate. Chou et al [3] investigated the effect of weave density and directional reinforcement on the mechanical fracture behavior, including Charpy impact strength of 3-D orthogonal non-woven composite. Chen et al [4] got the results of 3-D woven composites exhibited higher shear strength and impact energy absorption than 2-D woven composites. Chou et al [5, 6] studied impact energy absorption of three-axis or five-axis carbon fabric composites and found five-axis structures gave better impact strength compared to three-axis structures. Jenq et al [7] used FEM code MARC to calculate the impact energy absorption of 3-D braided composites based on the continuum assumption of the composite. Zikry and co-workers [8-14] conducted a series of researches on the damage mechanisms (including impact loading) of 3-D textile structural composites. Park et al [15] investigated the impact behaviors of 3-D woven composites with different Z-direction fiber length. Chiu et al [16] showed 3-D interlock woven composites exhibited a smaller impact damage area and higher residual strength than the 2-D woven laminated composites. Takatoya et al [17] obtained that lower in-plane properties and higher properties for open-hole and impact damage of 3-D textile composites. Gu et al [18-20] calculated the ballistic impact behavior of 3-D braided composite.

Above-mentioned studies ignore the strain rate effect on the mechanical properties of the 3-D textile composites because the 3-D textile composites are under high rate of loading when impact load is applied. To understand the strain rate effect on the mechanical behavior of composites, split Hopkinson pressure bar apparatus is often used in testing. Hosur et al [21-24] obtained the strain rate effect on the compressive behavior of different kinds of 3-D stitched composite. Sun et al [25-28] discussed the strain rate sensitivity of the compressive and tensile behavior of 3-D braided composite, 3-D woven composite and 3-D knitted composite.

However, the responses of high strain rate loading (including impact) on the 3-D woven structural composites are all studied in time domain so far. The rate sensitivity of the 3-D woven structural composites has not been investigated in frequency domain. The frequency response analysis of the 3-D woven structural composites under impact loading is another way and method to disclose the impact damage mechanisms and perhaps can find unknown behavior that hidden in time domain. The goals of this paper are to characterize rate sensitive compression behavior of the 3-D woven structural composites under different strain rate in frequency domain and to understand the relationship between input and output when the composite is treated as a system.

This paper will presents the frequency responses of 3-D angle-interlock woven composites under static (strain rate: 0.01/s) and impulsive (strain rate up to 2700/s) compression. The Z-transform method [29] will be employed to analyze the relationships between strain-time history and stress-time history of the composites. The amplitude and phase response of 3-D woven composite will be analyzed and compared. The factors that influence the system stability will also be discussed.

2 Application of Z-transform to 3-D woven structural composites

3-D woven structural composite can be regarded as a system. The strain-time history is input and stress-time history is output, or vice versa. The transfer function of the system reflects the constitutive relationship. Because the signals are sampled periodically for the compression test with MTS materials test system for quasi-static or the split Hopkinson pressure bar (hereafter referred as SHPB) apparatus, the strain-time history and stress-

time history are in discrete form and the composites can be regarded as discrete system.

2.1 Z-transform [29, 30]

The Z-transform was first introduced systematically by E.I.Jury in 1958 [31]. Assume $x(t)$ is the input and $y(t)$ is output for a system, it is well known that a linear discrete system can be described by the following difference equation:

$$b_0 y(n) + b_1 y(n-1) + \cdots + b_N y(n-N) =$$
$$a_0 x(n) + a_1 x(n-1) + \cdots + a_M x(n-M) \tag{1}$$

or

$$\sum_{k=0}^{N} b_k y(n-k) = \sum_{r=0}^{M} x(n-r) \tag{2}$$

where a_r and b_k are coefficients.

Taking unilateral Z-transform of the Equation 2 yields (Because the composite under compression could be regarded as a causal system. A causal system is a system with output and internal states that depends only on the current and previous input values.)

$$Y(z) \sum_{k=0}^{N} b_k z^{-k} = X(z) \sum_{r=0}^{M} a_r z^{-r} \tag{3}$$

and rearranging results in

$$H(z) = \frac{Y(z)}{X(z)} = \frac{\displaystyle\sum_{r=0}^{M} a_r z^{-r}}{\displaystyle\sum_{k=0}^{N} b_k z^{-k}} \tag{4}$$

where z is complex number and $H(z)$ is transfer function.

If such a system $H(z)$ is driven by a signal $X(z)$ then the output is $Y(z) = H(z)X(z)$. By performing partial fraction decomposition on $Y(z)$ and then taking the inverse Z-transform the output $y[n]$ can be found.

From the fundamental theorem of algebra the numerator has M roots (called zeros) and the denominator has N roots (called poles). The zeros of a Z-transform are the values of z for which $H(z) = 0$. The poles of a Z-transform are the values of z for which $H(z) = \infty$. Rewriting the transfer function in terms of poles:

$$H(z) = \frac{\left(1 - r_1 z^{-1}\right)\left(1 - r_2 z^{-1}\right) \cdots \left(1 - r_M z^{-1}\right)}{\left(1 - k_1 z^{-1}\right)\left(1 - k_2 z^{-1}\right) \cdots \left(1 - k_N z^{-1}\right)} \tag{5}$$

where r_k is the kth zero and k_k is the kth pole. The zeros and poles are commonly complex and when plotted on the complex plane it is called the

pole-zero plot. In simple words, zeros are the solutions to the equation obtained by setting the numerator equal to zero, while poles are the solutions to the equation obtained by setting the denominator equal to zero. In addition, there may also exist zeros and poles at $z = 0$ and $z = \infty$. If we take these poles and zeros as well as multiple-order zeros and poles into consideration, the number of zeros and poles are always equal.

The region of convergence (ROC) is where the Z-transform of a signal has a finite sum for a region in the complex plane.

$$ROC = \left\{ z : \sum_{r=0}^{\infty} x(n) z^{-n} < \infty \right\} \tag{6}$$

The stability of a system can also be determined by knowing the ROC. If the ROC contains the unit circle (i.e., $|z| = 1$) then the system is stable. And also, if the poles of $H(z)$ are within the unit circle, the system is stable; if the poles are out of the unit circle, the system is unstable; if the poles are on the unit circle, the system is under critical state.

The frequency response of a discrete system is the value of $H(z)$ at the unit circle:

$$H(z)\big|_{z=e^{j\omega}} = H(e^{j\omega}) \tag{7}$$

$$\because \ H(z) = \frac{Y(z)}{X(z)} = \frac{\sum_{r=0}^{M} a_r z^{-r}}{\sum_{k=0}^{N} b_k z^{-k}} = \sum_{n=-\infty}^{\infty} h(n) z^{-n} \tag{8}$$

$\therefore$ When $z = e^{j\omega}$:

$$H(e^{j\omega}) = \frac{Y(e^{j\omega})}{X(e^{j\omega})} = \frac{\sum_{r=0}^{M} a_r e^{-jr\omega}}{\sum_{k=0}^{N} b_k e^{-jk\omega}} = \sum_{n=-\infty}^{\infty} h(n) e^{-jn\omega} \tag{9}$$

Equation (9) can be written as:

$$H(e^{j\omega}) = \text{Re}(e^{j\omega}) + \text{Im}(e^{j\omega}) = \\ \left| H(e^{j\omega}) \right| \exp(j \arg[H(e^{j\omega})]) \tag{10}$$

where $\left| H(e^{j\omega}) \right|$ is amplitude and $\arg[H(e^{j\omega})]$ is phase.

2.2 Discrete system for 3-D woven structural composites and Z-transfrom

Assume $x(n)$ is strain-time history and $y(n)$ is stress-time history, and is input and output for the system repectively when the composite is regarded as a system. Because $x(n)$ and $y(n)$ are time series data sampled in testing, the composite is a discrete system. And also, the composite is assumed as a linear time-invariant (LTI) system. Furthermore, only the strain-time history or stress-time history before the failure time are considered because the composite will failure and become another system.

It can't use one difference equation to describe the discrete system of the 3-D textile structural composites under various strain rates because the composites are rate-sensitive materials [25-28]. For each strain rate, the system is simplified as a second-order and the following difference equation is used to characterize the discrete system for conciseness:

$$y(n) + b_1 y(n-1) + b_2 y(n-2) = \\ a_0 x(n) + a_1 x(n-1) + a_2 x(n-2) \tag{11}$$

The transfer function is:

$$H(z) = \frac{a_0 + a_1 z^{-1} + a_2 z^{-2}}{1 + b_1 z^{-1} + b_2 z^{-2}} \tag{12}$$

$H(z)$ can be obtained when strain-time history (input) and stress-time history (output) of the system are known. Then the frequency responses of the composite could be calculated from Equation 9 and 10. The stability of the composite in frequency domain can also be discussed from Equation 6.3 General Style Preferences

3 Materials and text methods

3.1 Materials

The weave construction of the 3-D angle-interlock woven fabric is shown in Fig.1. The E-glass filament tows without twists were employed to weave the 3-D angle-interlock fabric. The specification of the 3-D angle-interlock woven fabric is listed in Table 1. The vinyl ester resins were injected into the 3-D woven fabric preforms with RTM technique and then consolidated into 3-D woven fabric composites. The fiber volume fraction is about 40%. The thickness of the 3-D woven fabric composites is 3.0mm. The cross-section of the 3-D woven fabric composite is shown in Fig.2, where the binder yarns pass through the thickness direction can be observed. The composite coupons were cut and the in-plane size of composite coupon for compressive test is 9.0×9.0mm.
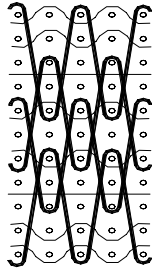
Fig.1 Architecture of 3-D woven fabric

Table 1 Main parameters of 3-D angle-interlock woven fabric

layers of warp/ weft			12/11
binding weave			O/L
number of warp		warp	816
		stuffer warp	272
		binding warp	544
		total number of warp	1632
number of warp per weave repeat			12
total number of weave repeat			136
weave parameters	warp density (ends/10*cm*)	total density	417.28
		average density per layer	34.77
	weft density (ends/10*cm*)	total density	993.73
		average density per layer	90.34
breadth (*cm*)			39.11
yarn number (*Tex*)		warp	168
		weft	254
fabric weight (g/100*cm*^{2})			33.2
fabric thickness (*mm*)		nominal	3.16
		after compress	2.92

Fig.2 Cross-section of 3-D angle-interlock woven composites

3.2 Compression tests

The composite coupons are compressed along two directions, which named as in-plane direction and out-of-plane direction, respectively. Quasi-static compression tests were conducted on MTS 810.23 materials test system at the compression speed of 0.1mm/min (strain rate of $10^{-3}s^{-1}$). The stress-time history and strain-time history could be obtained from test data.

High strain rate compressions were tested on split Hopkinson pressure bar (hereafter referred as SHPB) apparatus. The principle of the SHPB apparatus could be found elsewhere [32]. The strain rate differs from $600s^{-1} \sim 2700s^{-1}$ which depends on the impact velocity of striker bar [25, 26, 28]. If the modulus, cross section area and density of the bar are denoted by E_b, A_b and ρ_b and those of the specimen are E_s, As and ρ_s, the equations for the strain-rate($\dot{\varepsilon}$), strain (ε) and stress (σ) of the specimen are given by [32]:

$$\dot{\varepsilon}(t) = -\frac{2C_0}{L_s}\varepsilon_R(t) \tag{13}$$

$$\varepsilon(t) = -\frac{2C_0}{L_s}\int_0^t \varepsilon_R(t)dt \tag{14}$$

$$\sigma(t) = \frac{E_b A_b}{A_s}\varepsilon_T(t) \tag{15}$$

where $C_0 = \sqrt{E_b/\rho_b}$ is the longitudinal wave velocity in the bar, L_s is the specimen length, and $\varepsilon_R(t)$ and $\varepsilon_T(t)$ are the strain gage signal of the reflected and the transmitted pulses respectively. Equations (13) through (15) are based on the assumption that the dynamic forces on both sides of the specimen are equal and can be expressed as:

$$\varepsilon_I + \varepsilon_R = \varepsilon_T \tag{16}$$

Equations (14) and (15) give the strain-time history and stress-time history in composite specimen, i.e., the input and output of the discrete system.

4 Compression test results

Fig.3 is typical stress waves detected by the strain gages mounted on the incident and transmission bar of the SHPB apparatus along out-of-plane and in-plane direction respectively. From Equation 13 and 14, the strain rate vs. time history and strain-time history could be obtained. The strain rate vs. time history curves for out-of-plane and in-plane direction are shown in Fig.4. Fig.5 depicts the stress strain curves under quasi-static and high strain rates compression.
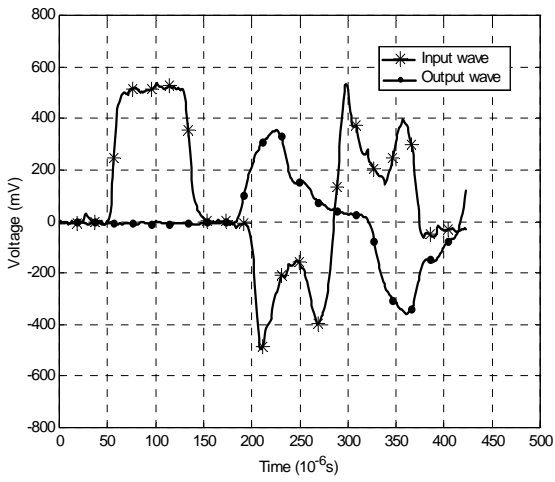
(a)
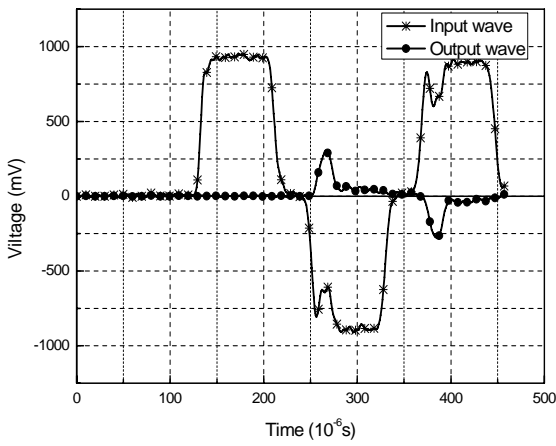
(b)

Fig.3 Typical input wave and output wave in SHPB apparatus for testing 3-D woven composite (a: out-of-plane compression   b: in-plane compression)
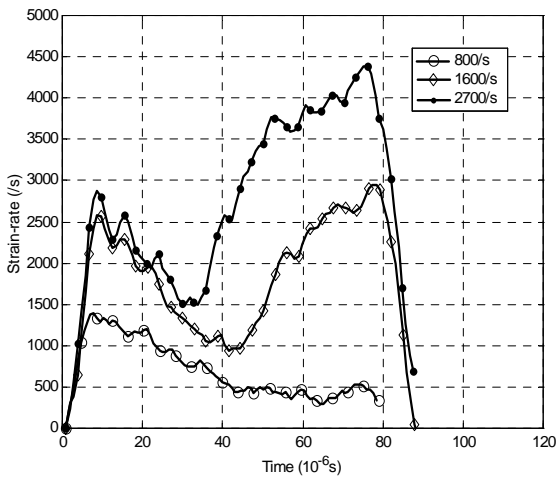
(a: out-of-plane compression)
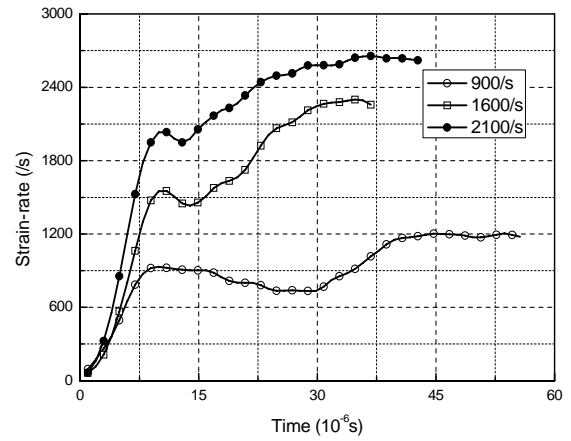
(b: in-plane compression)

Fig.4 Strain rate vs. time history of 3-D woven composite under high strain rate compression
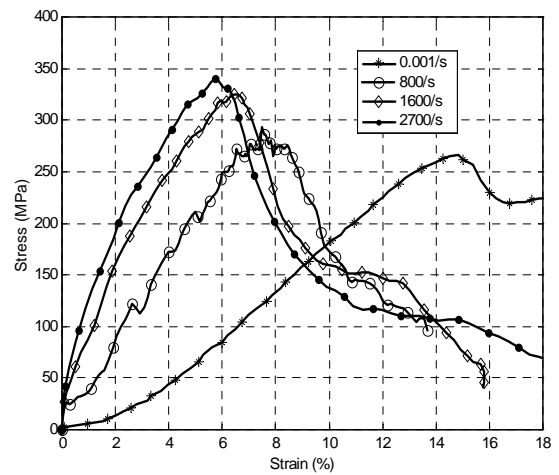
(a: out-of-plane compression)
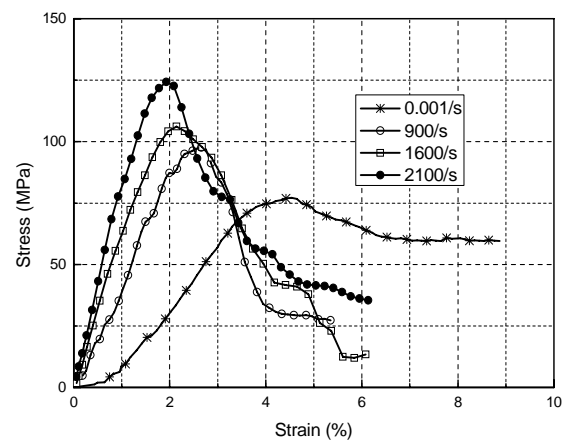
(b: in-plane compression)

Fig.5 Stress-strain curves of 3-D woven composite under various strain rates compression

5 Frequency responses and system stability of the 3-D textile structural composites

From the Equation 14, 15 and 16, the strain-time history and stress history could be obtained for high strain rate compression. For quasi-static compression, the two histories can also be obtained from MTS materials test system. Taking the composite specimen as a system, the transfer function and frequency response can be calculated from Equation 12 and 10. And from the poles of the system, the stability of the system can also be found.

The following equation is used to represent the difference equations of the system at quasi-static and high strain rates compression.

$$
\begin{bmatrix} 1 & b_{11} & b_{12} \\ 1 & b_{21} & b_{22} \\ 1 & b_{31} & b_{32} \\ 1 & b_{41} & b_{42} \end{bmatrix} \bullet \begin{bmatrix} y(n) \\ y(n-1) \\ y(n-2) \end{bmatrix} =
$$
$$
\begin{bmatrix} a_{10} & a_{11} & a_{12} \\ a_{20} & a_{21} & a_{22} \\ a_{30} & a_{31} & a_{32} \\ a_{40} & a_{41} & a_{42} \end{bmatrix} \bullet \begin{bmatrix} x(n) \\ x(n-1) \\ x(n-2) \end{bmatrix}
$$

(17)

where subscript i in $a_{i,j}$ and $b_{i,j}$ represents the difference equation coefficients at i^{th} strain rate, j is subscript has the same meaning with that in Equation 11.

5.1 Out-of-plane direction

The following difference equation is for out-of-plane compression at strain rates of 0.001/s, 800/s, 1600/s and 2700/s from upper row and lower row:

$$
\begin{bmatrix} 1 & -2.0516 & 1.0418 \\ 1 & -1.0182 & 0 \\ 1 & -0.942 & 0 \\ 1 & -0.09745 & 0 \end{bmatrix} \bullet \begin{bmatrix} y(n) \\ y(n-1) \\ y(n-2) \end{bmatrix} =
$$
$$
\begin{bmatrix} 1.2028 & -0.4411 & -1.0343 \\ 116.3852 & -190.2371 & 73.017 \\ 208.1948 & -336.4343 & 130.5079 \\ 322.6331 & -568.5773 & 246.1609 \end{bmatrix} \bullet \begin{bmatrix} x(n) \\ x(n-1) \\ x(n-2) \end{bmatrix}
$$

(18)

The comparison of stress-strain curves between experimental and fitted from Equation 18 is shown in Fig.6. There are good agreements between experimental and prediction. It is proven that the assumptions for the discrete system of composite are appropriate for Z-transform.
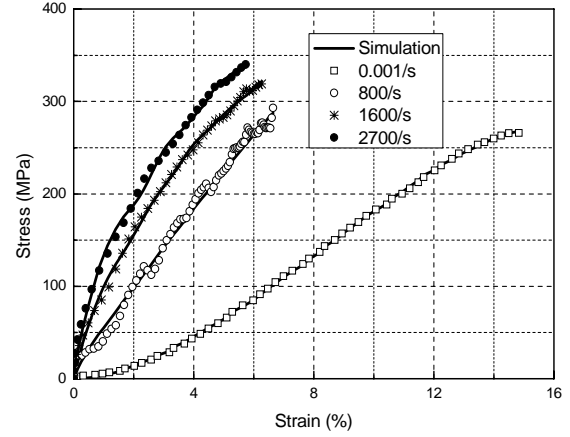
Fig.6 Comparison of stress strain curves of 3-D woven composite under out-of-plane compression between experimental and system prediction

The amplitude and phase responses of the difference equation 18 could be obtained from Equation 12 and 10. The amplitude and phase responses are shown in Fig.7 and Fig.8 respectively. The abscissa is normalized frequency (unit: $\times \pi rad / sample$) for Fig.7 and Fig.8, and the ordinate is relative amplitude in Fig.7 (unit: dB).
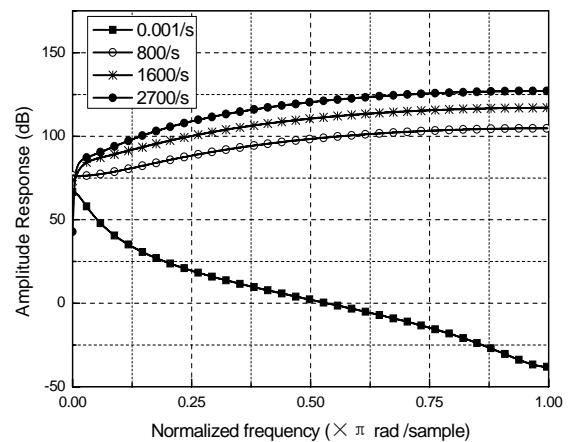
Fig.7 Amplitude response of 3-D woven composite under out-of-plane compression at various strain rates
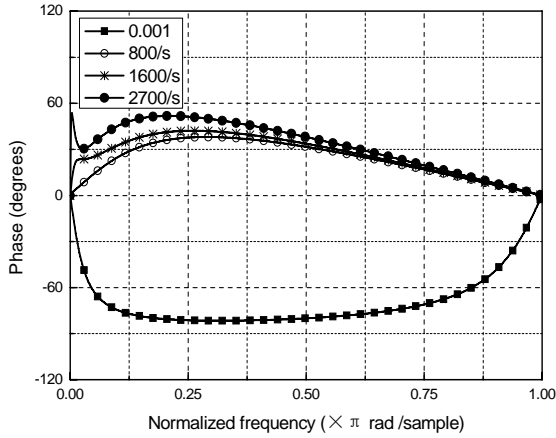
Fig.8 Phase response of 3-D woven composite under out-of-plane compression at various strain rates

For the amplitude response in Fig.7, the amplitudes under four strain rates are almost equal. Then the amplitude decreases with normalized frequency at quasi-static state and increases with normalized frequency at high strain rate state.

For the phase response in Fig.8, the phase is negative for quasi-static loading and positive for high strain rate loading. At the same normalized frequency, the phase increases with strain rate. At the same strain rate, the phase increases first and then decreases.

The distribution of poles in Z-plane is used judge the stability of transfer function of the 3-D woven composite. Fig.9 is the distribution at different strain rates. The abscissa is real part of poles and the ordinate is imaginary part of poles. The cross symbol of '×' are poles. The poles are outside of unit circle for quasi-static compression which means the unstable system and completely within the unit circle when strain rate is up to 1600/s which means stable system. For the strain rate of 2700/s, the poles are located near the center of unit circle, which means the system is more stable than that of 1600/s. For the same material and same initial state of test (zero compression stress before testing), only the strain rate (different loading conditions) influences the system stability.

(a) 0.001/s (b) 800/s

(c) 1600/s (d) 2700/s
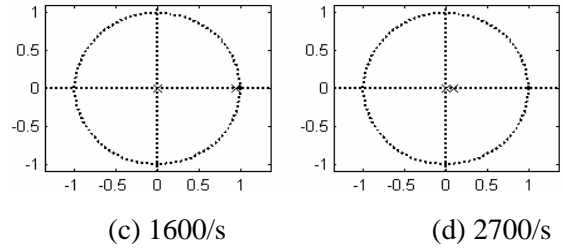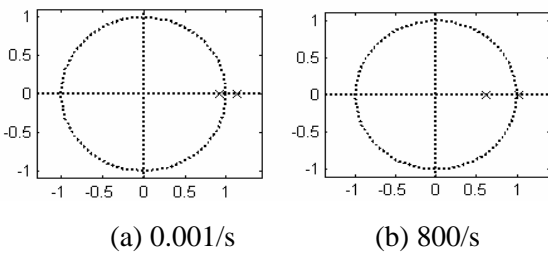
Fig.9 Poles distribution for out-of-plane direction

5.2 In-plane direction

For the in-plane compression of 3-D woven composite under quasi-static and high strain rate compression, the difference equation is as follows for strain rates of 0.001/s, 900/s, 1600/s and 2100/s from upper row to lower row:

$$\begin{bmatrix} 1 & -2.0256 & 1.0344 \\ 1 & -2.0197 & 1.0505 \\ 1 & -1.1284 & 0 \\ 1 & -1.1712 & 0 \end{bmatrix} \bullet \begin{bmatrix} y(n) \\ y(n-1) \\ y(n-2) \end{bmatrix} =$$
$$\begin{bmatrix} 3.2964 & -5.5156 & 2.2863 \\ 31.5499 & -62.0476 & 31.5959 \\ 43.4288 & -18.9157 & -36.2463 \\ 68.4742 & -54.4938 & -32.5118 \end{bmatrix} \bullet \begin{bmatrix} x(n) \\ x(n-1) \\ x(n-2) \end{bmatrix} \qquad (19)$$

The discrete system can also fit the stress strain curve precisely shown in Fig.10. Fig.11 and Fig.12 are the amplitude and phase responses respectively. The amplitude has a peak point for 0.001/s and a deep valley for 900/s. This phenomenon depends on the poles location in the Z-plane. According to the Z-transform theory [30], the amplitude responses will have a deep valley if poles are near the center point or zeros are near the unit circle, and will have a peak point if poles are near unit circle. At the same normalized frequency, the amplitude increases with the strain rate; at the same strain rate for 1600/s and 2100/s, the amplitude decrease with the increase of normalized frequency.
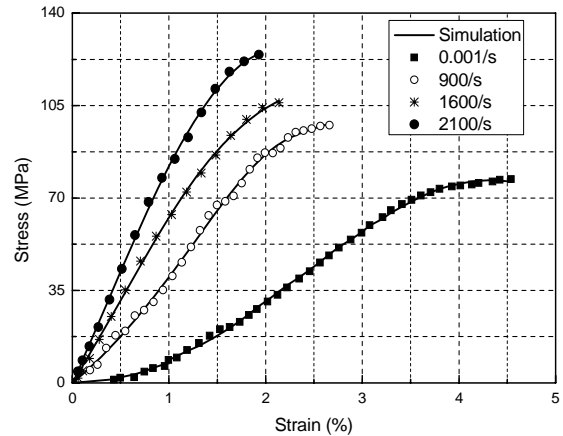
Fig.10 Comparison of stress strain curves of 3-D woven composite under in-plane compression between experimental and system prediction
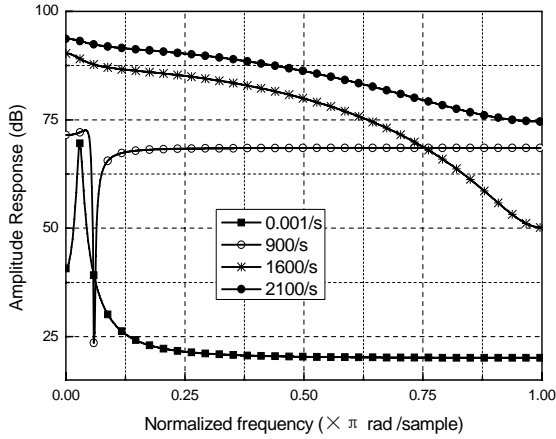
Fig.11 Amplitude response of 3-D woven composite under in-plane compression at various strain rates
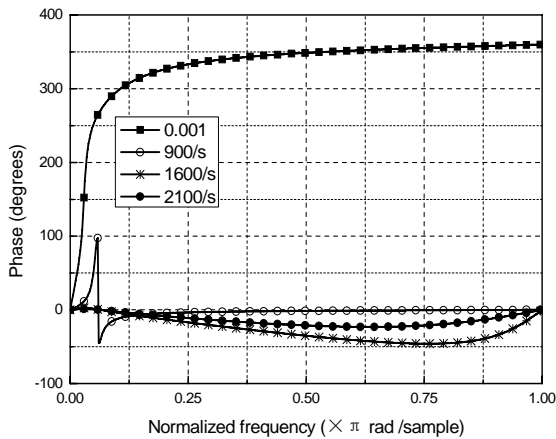
Fig.12 Phase response of 3-D woven composite under in-plane compression at various strain rates

From Fig.13 of poles distribution, it is obviously that the system becomes unstable as the strain rate increases. The instability is attributed to the unstable damage under in-plane compression as compared with that under out-of-plane compression at strain rate of 1600/s (Fig.14).

(a) 0.001/s   (b) 900/s

(c) 1600/s   (c) 2100/s
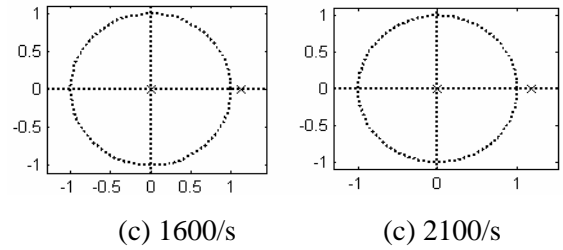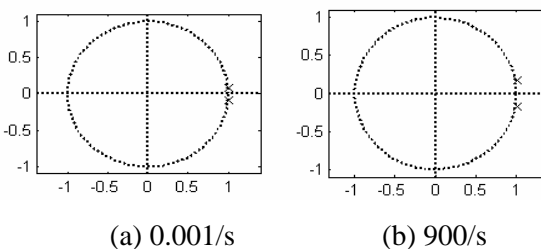
Fig.10 Poles distribution for in-plane direction
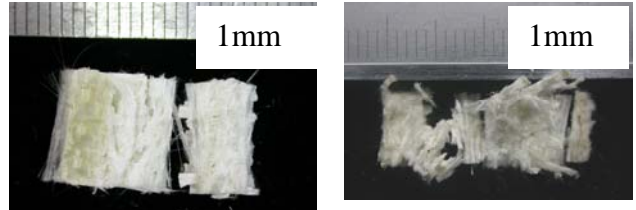
Fig.14 Comparison of compressive damage of 3-D woven composite at strain rate of 1600/s
(left: out-of-plane direction   right: in-plane direction)

6 Discussions

1) The Z-transform plays the same role in the analysis of discrete-time signals and linear time-invariant (LTI) systems as the Laplace transform does in the analysis of continuous-time signals and LTI systems. For example, we shall see that in the Z-domain (complex Z-plane) the convolution of two time-domain signals is equivalent to multiplication of their corresponding Z-transform. This property greatly simplifies the analysis of the response of an LTI system to various signals. In addition, the Z-transform provides us with a means of characterizing an LTI system, and its response to various signals, by its pole-zero locations. This paper employs the Z-transform to analyze the sampled data of the 3-D woven structural composites under quasi-static and high strain rate compression. The composites are regarded as a system. The transfer function of the system resembles the constitutive relationship if the strain-time history is an input and the stress-time history is an output of the system, or vice versa. From the Z-transform, the mechanical property of the composite could be studied at the frequency domain. This paper is an attempt.

2) For a certain composite material, there is a certain frequency response. From the amplitude and phase responses, the transfer function of the system can be converted. The discrete transfer function of a system can be optimized by a command of "invfreqz" in Matlab® when the difference equation is known. The stability of the system described by the difference equation can be improved after

optimization. Because the stability of the transfer functions remains the same before and after optimization, it could be concluded that the stability or instability of a system only depends on the materials' properties and testing condition.

3) The relationships among the system stability and microstructure, mechanical behavior of composite materials are still unknown so far. The factors which influence the system stability can be analyzed qualitatively as follows:

i) Strain rate: There is sufficient time for stress propagated to all flaws in the composites under quasi-static compression. The accumulative damage in materials depends on the formation of all cracks and flaws. As the strain rate increases, there is no sufficient time for stress waves reach flaws. The damage of composite is controlled by relatively small amount of flaws. Then system will become stable at high strain rate.

ii) Microstructure: As the strain rate of out-of-plane compression increases, the damage only occurred at the local parts of tows in thickness direction unlike contrary to that in quasi-static compression. The 3-D woven composite will become more stable under high strain rate compression along out-of-plane direction. For the in-plane compression, there are contrary tendency because of microstructure deformation.

4) The Z-transform can be extended to research other behaviors of composite materials, not only for mechanical properties and fiber reinforced composites. For example, the application of Z-transform to composite materials by Gao et al [33] is to investigate interactions between solid/solid interfaces, including charge transfer through diodes and molecular wires. In particular, the Z-transform can be applied, using the tight-binding wave functions, to study the interface between a ''molecular wire'' and a metallic surface and the contact between nanotubes and metals.

7 Concluding remarks

The out-of-plane and in-plane compression behaviors and frequency responses of 3-D woven structural composites have been compared both under quasi-static state (tested with MTS materials test system) and high strain rate state (tested with SHPB apparatus) in frequency domain. Taking the composites as discrete systems, the difference equations and transfer functions have been obtained. The Z-transform is used to analyze the frequency responses and system stability. The good agreements of stress-strain curves between experimental and fitted results from difference equation of the discrete system prove the validation of assuming the composite is a discrete system.

For 3-D woven composite, the amplitude and phase responses increase with strain rate at in-plane and out-of-plane compression; and the discrete system of the woven composite becomes more stable at in-plane compression and unstable at in-plane compression as strain rate increases.

From the comparison among system stability for 3-D woven structural composites, it is shown that microstructure of composites and strain rate influence the system stability. Further studies should be conducted to investigate the relationships among mechanical behaviors, damage modes, frequency reposes of the discrete system and system stability for the 3-D woven structural composites under quasi-static and high strain rate compression.

References

[1] Ko FK, Hartman D. Impact behavior of 2-D and 3-D glass-epoxy composites. SAMPE Journal. 22 (4): 26-30 1986

[2] Gong JC, Sankar BV. Impact properties of 3-dimensional braided graphite epoxy composites. Journal of composite materials. 25 (6): 715-731 1991

[3] Chou S, Chen HC, Chen HE. Effect of weave structure on mechanical fracture-behavior of 3-dimensional carbon-fiber fabric reinforced epoxy-resin composites. Composites science and technology. 45 (1): 23-35 1992

[4] Chen HP, Jang BZ. Failure mechanisms of 2-D and 3-D woven fiber-reinforced polymer composites. Polymer composites. 16 (2): 125-134 1995

[5] Chou S, Chen HE, Song MS. A study on impact properties of 3-D composites by falling weight test method. Journal of the Chinese institute of engineers. 19 (1): 25-34 1996

[6] Chou S, Chen HE. Effects of structure and microcracks on the flexure, interlaminar shear and impact properties of three-dimensional composites. Polymers & polymer composites 4 (6): 387-395 1996

[7] Jenq ST, Kuo JT, Sheu LT. Ballistic impact response of 3-D four-step braided glass/epoxy composites. Key engineering materials. 141-1: 349-366 Part 1-2 1998

[8] Flanagan MP, Zikry MA, Wall JW, El-Shiekh A. An experimental investigation of high velocity impact and penetration failure modes in textile composites. Journal of composite materials. 33 (12): 1080-1103 1999

[9] Bahei-El-Din YA, Zikry MA. Impact-induced deformation fields in 2D and 3D woven composites. Composites science and technology. 63 (7): 923-942 2003

[10] Bahei-El-Din YA, Zikry MA, Rajendran AM. Impact-induced deformation fields in 3D cellular woven composites. Composites Part A, 34 (8): 765-778 2003

[11] Baucom JN, Zikry MA. Evolution of failure mechanisms in 2D and 3D woven composite systems under quasi-static perforation. Journal of composite materials. 37 (18): 1651-1674 2003

[12] Baucom JN, Zikry MA, Qiu Y. Dynamic and quasi-static failure evolution of 3D woven cellular composite systems. Journal of reinforced plastics and composites. 23 (5): 471-481 2004

[13] Baucom JN, Zikry MA. Low-velocity impact damage progression in woven E-glass composite systems. Composites Part A. 36 (5): 658-664 2005

[14] Baucom JN, Zikry MA, Rajendran AM. Low-velocity impact damage accumulation in woven S2-glass composite systems. Composites science and technology. 66 (10): 1229-1238 2006

[15] Park SJ, Park WB, Lee JR. Characterization of the impact properties of three-dimensional glass fabric-reinforced vinyl ester matrix composites. Journal of materials science. 35 (24): 6151-6154 2000

[16] Chiu CH, Lai MH, Wu CM. Compression failure mechanisms of 3-D angle interlock woven composites subjected to low-energy impact. Polymers & polymer composites. 12 (4): 309-320 2004

[17] Takatoya T, Susuki I. In-plane and out-of-plane characteristics of three-dimensional textile composites. Journal of composite materials, 39 (6): 543-556 2005

[18] Gu BH, Li YL. Ballistic perforation of conically cylindrical steel projectile into three-dimensional braided composites. AIAA Journal. 43 (2): 426-434 2005

[19] Gu BH, Ding X. A refined quasi-microstructure model for finite element analysis of three-dimensional braided composites under ballistic penetration. Journal of composite materials. 39 (8): 685-710 2005

[20] Lian J, Gu BH. Ballistic impact simulation of 3-D rectangular braided composite struck by steel projectile at microstructure level. International journal of nonlinear sciences and numerical simulation. 7 (3): 313-316 2006

[21] Hosur MV, Abraham A, Jellani S, Vaidya UK. Studies on the influence of through-the-thickness reinforcement on low-velocity and high strain rate response of woven S2-glass/vinyl ester composites. Journal of composite materials. 35 (12): 1111-1133 2001

[22] Hosur MV, Adya M, Vaidya UK, Mayer A, Jeelani S. Effect of stitching and weave architecture on the high strain rate compression response of affordable woven carbon/epoxy composites. Composite structures. 59 (4): 507-523 2003

[23] Hosur MV, Karim MR, Jeelani S. Experimental investigations on the response of stitched/unstitched woven S2-glass/SC15 epoxy composites under single and repeated low velocity impact loading. Composite structures. 61 (1-2): 89-102 2003

[24] Hosur MV, Karim MR, Jeelani S. On the response of stitched woven S2-glass/epoxy composites to high strain rate compression loading. Polymers & polymer composites. 12 (3): 183-196 2004

[25] Sun BZ, Gu BH, Ding X. Compressive behavior of 3-D angle-interlock woven fabric composites at various strain rates. Polymer testing. 24 (4): 447-454 2005

[26] Sun BZ, Liu F, Gu BH. Influence of the strain rate on the uniaxial tensile behavior of 4-step 3D braided composites. Composites Part A. 36 (11): 1477-1485 2005

[27] Sun BZ, Yang L, Gu BH. Strain rate effect on four-step three-dimensional braided composite compressive behavior. AIAA Journal. 43 (5): 994-999 2005

[28] Sun BZ, Hu H, Gu BH. Compressive behavior of multi-axial multi-layer warp knitted (MMWK) fabric composite at various strain rates. Composite structures. 2007,pp.84-90

[29] Robert Vich. Z transform theory and applications [Chapter 6: Application of the Z transform to the analysis of discrete signals]. D. Reidel Publishing Compacy, Holland, 1987, pp.187-216

[30] John G. Proakis, Dimitris G. Manolakis. Digital signal processing (4th edition) [Chapter 3: The Z-transform and its application to the analysis of LTI systems]. Pearson Education Inc, Pearson Prentice Hall, New Jersey 07458, 2007, pp. 147-223

[31] Eliahu I. Jury. Sampled-data control systems [Chapter 1: Z-transform method for analysis; Chapter 2: Modified Z-transform method]. John Wiley & Sons, New York, 1958, pp.1-118

[32] Marc A. Meyers. Dynamic behavior of materials [Chapter 12: Experimental techniques: Methods to

produce dynamic formation], New York: John Wiley & Sons, Inc., 1994, pp. 296-322

[33] Gao YQ, Marcus RA. Application of the Z-transform to composite materials. Journal of chemical physics. 115 (21): 9929-9934 2001